

# Fuzzy Logic Controller based PV System Connected in Standalone and Grid Connected Mode of Operation with Variation of Load

B.Krishna Naick\*<sup>‡</sup>, T.K.Chatterjee\*\*, K.Chatterjee\*\*\*

\* & \*\*\* Department of Electrical Engineering, Faculty of Electrical Engineering, Indian Institute of Technology (ISM), Dhanbad, Jharkhand, India-826004.

\*\*Department of Mining Machinery Engineering, Faculty of Mining Machinery Engineering, Indian Institute of Technology (ISM), Dhanbad, Jharkhand, India-826004.

(krishnalalitha.b@gmail.com, tkcism@yahoo.com, kalyanbit@yahoo.co.in)

<sup>‡</sup> Corresponding Author; B.Krishna Naick, Faculty of Electrical Engineering, Department of Electrical Engineering, Indian Institute of Technology (ISM), Dhanbad, Jharkhand, India-826004. Tel: +91 326 223 5654,

Fax: +91 326 229 6563, krishnalalitha.b@gmail.com

*Received: 07.11.2016 Accepted:22.12.2016*

**Abstract-** Solar photovoltaic (PV) system has gained its own importance in global electrical power generation. The increase in efficiency of PV cell, due to improvement in design parameters has led the world to use solar PV system as one of the reliable alternative energy source. PV system may be connected either in standalone mode or grid connected mode along with single stage configuration or two stage configuration. The intermediate stages present between solar PV system and grid is the boost converter with maximum power point (MPP) tracking controller and the inverter with different control techniques. The present work explains about a 14 kW and 10 kW solar PV system of two stage configuration simulated in standalone mode and grid connected mode with simple proportional-integral (PI) controller and fuzzy logic controller (FLC) to regulate dc output voltage. The behavior of PV system has been observed with switching on of an additional load for a stipulated time period. The performance of solar PV system under disparate running conditions and its associated power curves were presented.

**Keywords** PV system, Fuzzy logic controller, PI controller, standalone mode, grid connected mode.

## 1. Introduction

The growth in demand and consumption of electrical energy has increased the usage of conventional fuels to generate electrical energy, leading to growing concern of its impact on environmental aspects which led policy makers to emphasize more on alternative sources of energy. Of all types, solar energy is easily available and it may be harnessed on a large scale irrespective of any site. Solar energy may be harnessed in small, medium and large scale depending upon the load requirements [1]. Solar energy is vastly harnessed in medium scale near to the load centre and after meeting load requirements, the excess power will be supplied to the grid. The two stage configuration of solar PV system includes a suitable dc-dc conversion system with maximum power point (MPP) tracking controller and a dc-ac

conversion unit [2]. The efficiency of power electronic systems, its transient stability, active and reactive power control in two stage conversion system plays an important role and hence, the maximum effort is on improving these parameters [2].

To yield maximal power from PV array during environmental variations such as temperature and solar insolation, dc-dc converter with MPP tracking system is being employed. Several types of MPP tracking algorithms are reported in [3]. A comparative study on different MPP tracking techniques based on their complexities, ease of hardware realization, advantages, disadvantages and application were discussed in [4,5]. Perturb and observe (P&O), incremental conductance (INC), hill climbing (HC),

parasitic capacitance, constant voltage and current methods are some of the famous and conventional techniques.

Among the reported techniques, it is easy to implement P&O and INC methods of MPP tracking owing to their inherent advantages. The P&O based MPP tracking method is a low cost method, but fails to track optimal power point under sudden variations in atmospheric conditions leading to fluctuations in the operating point due to which some amount of energy is wasted [6]. Modifications based on several optimization algorithms have been suggested, however it has been reported that the controller response is slow and will cause overall decrease in efficiency [6]. On other hand, INC method is the second highly popular method in tracking the MPP. However, in comparison with P&O or the HC technique, the INC algorithm is little bit complicated [7]. Advanced intelligent MPP tracking control techniques have been established, but they are having their own limitations in implementation. Most of the MPP tracking techniques are employed to regulate the duty ratio of dc-dc converter topologies.

A dc-dc converter along with MPP tracking controller is the first stage of configuration, which will be present between PV array and inverter. To realize standalone and grid connected mode of operation of PV system through dc-ac converter, an appropriate dc voltage level is required, which may be achieved by employing suitable dc-dc converter topologies.

Switched mode dc-dc converters, widely used in dc supply system, are considered to be the main part in MPP tracking system. The purpose of converters is to maintain the voltage at an appropriate level at the input side of inverter and to run the PV array at MPP. The converter will try to match the internal impedance and external impedance of PV array so that the maximum power will be yielded at the time of uncertainty in environmental conditions. The impedance matching depends upon the duty cycle fed by MPP tracking controller and conversion efficiency of dc-dc converter. Recently, the intelligent control techniques like artificial neural network (ANN) and fuzzy logic controller (FLC) has gained wide popularity because of their reliable operation. ANN and FLC based MPP tracking were explained in [8].

Control of power quality, regulation of dc voltage and reliability of power are the major issues for large scale connection of PV system to the grid. Relative power present between input and output side, dc link voltage and temperature will effect the conversion efficiency of an inverter. In order to have control over the quality of power fed to grid, two or multi-level voltage source inverter (VSI) with different pulse width modulation (PWM) control techniques were being utilized by the researchers around the world. The power flow between PV system and the utility will be controlled by operating the VSI in voltage or current control mode. The dc voltage regulator and current controller are considered to be an important components in an inverter control strategy. The proper mode of operation of VSI may also be initiated during fault conditions for an islanding purpose [9].

Different types of linear and non-linear controllers were found in literature. Current controllers are realized using linear and conventional controllers like PI (proportional and integral) or other control techniques like hysteresis, predictive and sliding mode control to limit harmonic content and power factor of current fed to grid [10]. The main problem with PI controller lies in tuning its gain values with respect to changes in atmospheric condition and the other problems associated with them are harmonics, conversion efficiency and electromagnetic interference due to higher switching frequencies [10].

Therefore, in present work, FLC (a non-linear controller) has been implemented in dc voltage regulation block and the results thus obtained were analyzed with respect to the results obtained from conventional PI controller. The rest part of paper has been arranged in the following manner. Section 2 explains about the modeling of PV module. Section 3 deals with boost converter and P&O algorithm based MPP tracking. Implementation of conventional PI controller and FLC in voltage regulator block of inverter controller circuit have been discussed in section 4. The implementation of Simulink model and results were explained in section 5 and section 6.

## 2. Modeling of Solar PV System

The physical modelling of solar PV system has been discussed in this section. The PV cell is a simple semiconductor material which produces electricity when exposed to solar radiation. Electrical behaviour of solar PV cell is represented in the form of mathematical models like single diode and two diode equivalent model [11, 12]. Out of these models, single diode equivalent model as shown in "Fig.1" was found to be best with less complexity, higher efficiency and easier to implement.

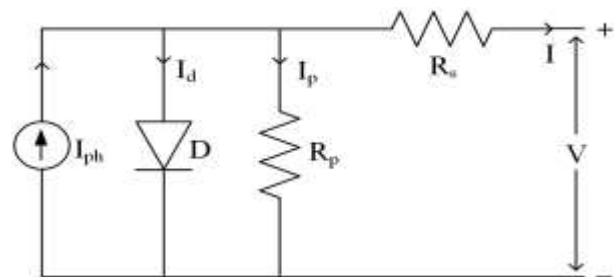


Fig. 1. Single diode equivalent model.

The output current  $I$  of PV module is expressed by (1) [11].

$$I = I_{ph} - I_0 \left[ \exp \left( \frac{V + IR_s}{V_t a} \right) - 1 \right] - \frac{V + IR_s}{R_p} \quad (1)$$

$I_0$  is the reverse saturation current,  $V$  is the output voltage,  $a$  is the diode ideality factor,  $R_s$  and  $R_p$  are the equivalent series and parallel resistance,  $V_t$  is the thermal voltage of PV array and is given by  $V_t = N_s k T / q$ .  $N_s$  represents the number of series connected cells in a string of PV module,  $k$  is the Boltzmann constant (and is equal to  $1.3806503 \times 10^{-23} \text{ J/K}$ ),  $T$  is the temperature at the

*p-n* junction of PV cell given in kelvin, *q* is electron charge and its value is  $1.60217646 \times 10^{-19} \text{C}$ . The current  $I_{ph}$  generated by PV module due to incident of solar irradiation is expressed in (2).

$$I_{ph} = (I_{sc} + K_T \Delta_T) \frac{G}{G_n} \quad (2)$$

$I_{sc}$  is the short circuit current or current generated by PV cell at nominal temperature of 25°C and standard solar irradiation of 1000 W/m<sup>2</sup>,  $K_T$  stands for the short circuit current temperature coefficient,  $\Delta_T$  is the difference in actual and nominal temperature of PV module in kelvin and is also given by  $\Delta_T = T - T_n$ , whereas  $T_n$  and  $T$  are the nominal and actual operating temperature in kelvin.

$G$  and  $G_n$  (in W/m<sup>2</sup>) are the solar irradiation at normal operating conditions and at nominal temperature. The reverse

saturation current is dependent upon temperature and is stated by (3).

$$I_0 = I_{n0} \left(\frac{T_n}{T}\right)^3 \exp\left[\frac{qE_g}{ak} \left(\frac{1}{T_n} - \frac{1}{T}\right)\right] \quad (3)$$

$E_g$  is the bandgap energy of semiconductor material and its value is 1.12 eV for polycrystalline silicon at 25°C.  $I_{n0}$  is the saturation current at nominal temperature and it is expressed by (4).

$$I_{n0} = \frac{I_{sc}}{\exp(V_{oc}/a V_{nt}) - 1} \quad (4)$$

$V_{oc}$  is the open circuit voltage at nominal temperature and  $V_{nt}$  is the thermal voltage produced by  $N_s$  cells connected in series in one string of array at nominal temperature.

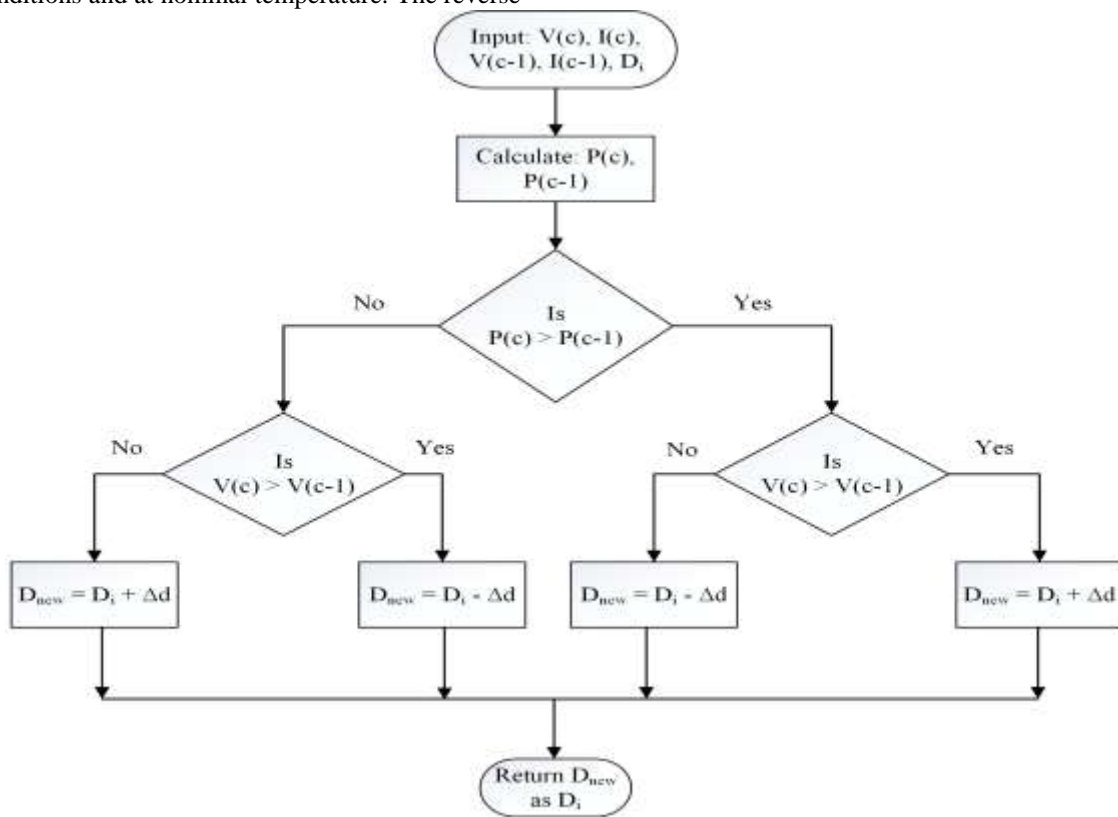


Fig. 2. Flow diagram of P&O algorithm.

**3. Boost Converter and MPP Tracking**

Insolation of sun varies from time to time throughout the day and it is very important to extract maximum possible power from PV array, which produces power as per insolation level. For high voltage application, the boost converter is considered suitable and it has been employed between PV array and dc-ac converter. The main function of dc-dc converters is to match load resistance with input resistance of PV array in order to generate maximum power according to maximum power transfer theorem [13] and for this purpose the MPP tracking controller has been employed. The main objective of MPP tracking method is to calculate suitable duty cycle  $D_i$ , which acts as input to the switch employed in boost converter. In this paper, the P&O method

based MPP tracking has been implemented to compute the duty ratio and its flow diagram is shown in “Fig.2”.

The relation between input voltage  $V_i$ , output voltage  $V_o$  and duty cycle  $D_i$  of boost converter is expressed in (5) [14].

$$V_o = \frac{V_i}{(1-D_i)} \quad (5)$$

In P&O MPP tracking method, voltage (V) and current (I) is sensed at the current step ( $c^{th}$ ) and the previous step ( $(c-1)^{th}$ ) and corresponding PV power (P) will be calculated and compared. If power at current step is greater than that of power at the previous step, the perturbation will continue in the present direction, or else it will be carried out in opposite direction by updating the duty cycle (by an amount  $\pm\Delta d$ ) from  $D_i$  to new duty cycle.

Hence, based on comparison of power and direction of perturbation, there will be increase or decrease in the value of duty cycle with small step. The advantages of this method are that it is easier to implement and MPP may be quickly achieved. The disadvantage associated with this method is that there will be always fluctuation at MPP tracking point and it will never reach optimal point because of its perturbation nature [6]. To deal with the above disadvantages, an adaptive P&O method has been proposed in [15]. Authors in [16] have presented an adaptive P&O method with FLC which offers stable, fast and better transient response in comparison to basic P&O method.

**4. Inverter Control Strategy**

*4.1. Implemented Controller*

In present model, the solar PV system has been simulated in isolated mode and grid connected mode in two stages. The first stage is associated with the boost converter, here PV array voltage is increased to higher value and is driven at MPP level. The second stage is conversion of power from dc to three phase ac system, so that it may be

suitably integrated to grid and also for supplying the connected load. Inverter is considered to be an important part in interfacing the PV system to grid. Driving an inverter at a suitable value will control the active and reactive power to be produced and supplied to grid. The reactive power should be limited to a suitable minimum value or zero value, with the help of controller circuit. If reactive power is required by the load, it will draw the same from grid. In standalone mode of PV system, a simple controller circuit as shown in “Fig. 3” was implemented so that only active power is produced by the inverter.

From “Fig.3”, it may be observed that input voltages of load is measured and park’s transformation as in (6) is implemented to transform input abc voltages to synchronous reference frame dq0 components and its inverse as in (7) is used to generate output reference voltage for producing controlled switching pulses of an inverter. The measured load voltage is compared with reference voltage and corresponding error is generated. The PI controller minimizes error and generates controlled output reference voltage, which is fed to pulse width modulation (PWM) generator. The park’s transformation and its inverse transformation equations are given in (6) and (7).

$$\begin{bmatrix} V_d \\ V_q \\ V_0 \end{bmatrix} = \frac{2}{3} \begin{bmatrix} \cos(\theta) & \cos(\theta - \frac{2\pi}{3}) & \cos(\theta + \frac{2\pi}{3}) \\ -\sin(\theta) & -\sin(\theta - \frac{2\pi}{3}) & -\sin(\theta + \frac{2\pi}{3}) \\ \frac{1}{2} & \frac{1}{2} & \frac{1}{2} \end{bmatrix} \begin{bmatrix} V_a \\ V_b \\ V_c \end{bmatrix} \tag{6}$$

$$\begin{bmatrix} V_a \\ V_b \\ V_c \end{bmatrix} = \begin{bmatrix} \cos(\theta) & -\sin(\theta) & 1 \\ \cos(\theta - \frac{2\pi}{3}) & -\sin(\theta - \frac{2\pi}{3}) & 1 \\ \cos(\theta + \frac{2\pi}{3}) & -\sin(\theta + \frac{2\pi}{3}) & 1 \end{bmatrix} \begin{bmatrix} V_d \\ V_q \\ V_0 \end{bmatrix} \tag{7}$$

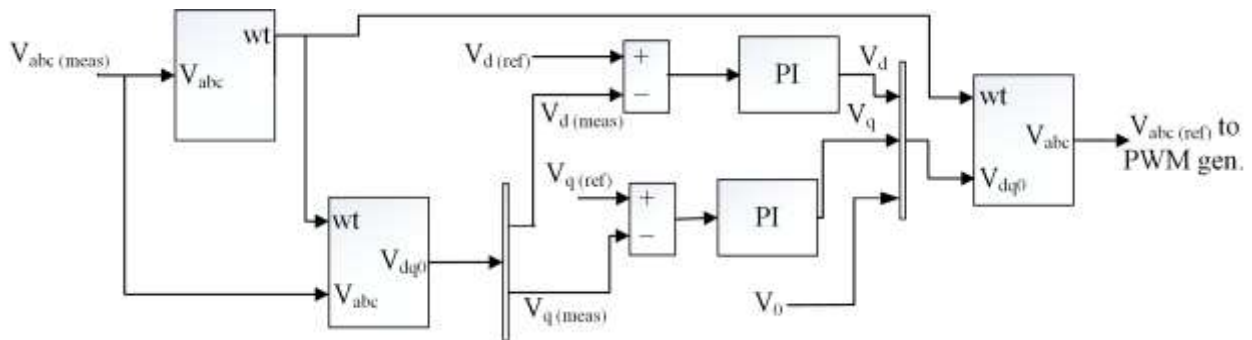


**Fig. 3.** Controller circuit of an inverter in isolated mode of operation of PV system.

In standalone and grid connected mode of PV system, the controller is employed with voltage regulator and current controller to produce reference output voltage which is being fed to PWM generator. The objective is to study output voltage stability of inverter with changes in load by implementing PI controller and FLC in voltage regulator block of controller circuit in an inverter.

The controller circuit of an inverter is shown in “Fig. 4”. Instead of measuring load voltage and current, grid voltage and current have been measured and is fed to current controller circuit. The R and L represents resistance and

inductance values at interface point between PV system and grid. The voltage regulator block generates synchronous reference current  $I_d^*$  which is provided as input to current controller block. The FLC based voltage regulator block is shown in “Fig. 5”.

The equations implemented in current controller circuit is given by (8) and (9) [21].

$$V_{dr} = V_{d(meas)} + I_d^*R - I_qL + d(I_d^*) \tag{8}$$

$$V_{qr} = V_{q(meas)} + I_d^*L + I_qR + d(I_q) \tag{9}$$

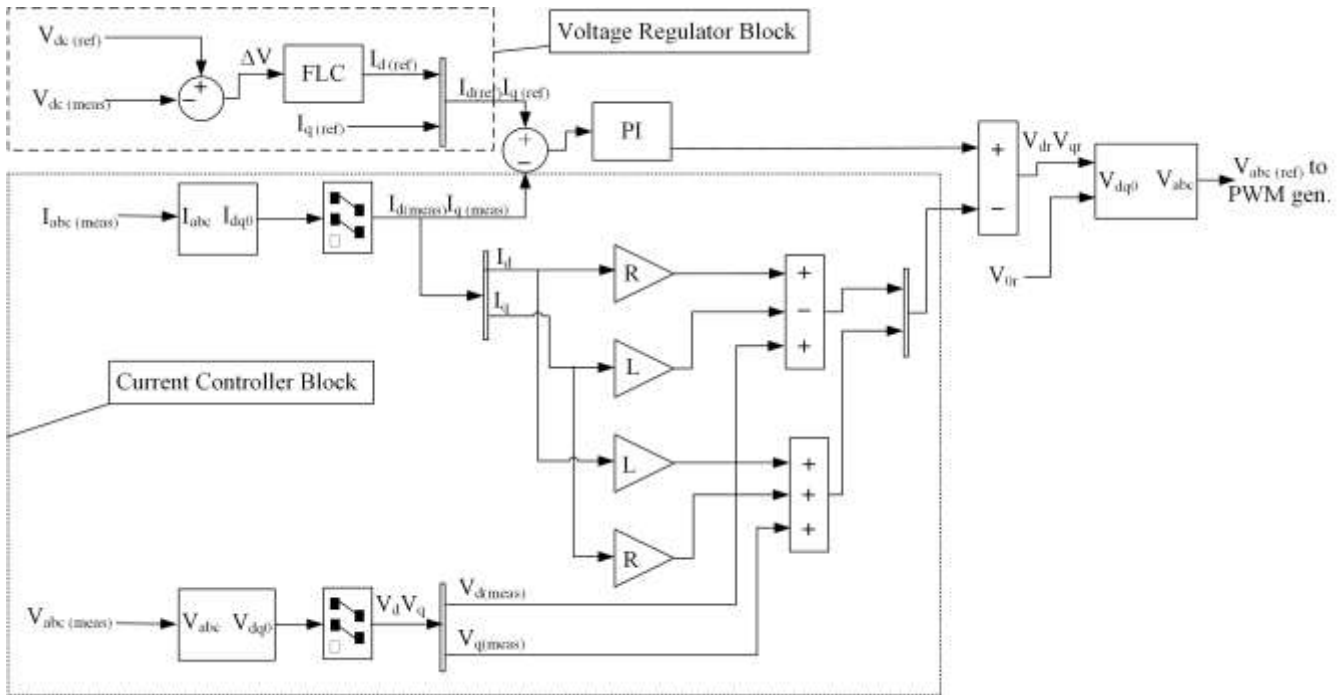


Fig. 4. Controller circuit of an inverter in isolated mode of operation of PV system.

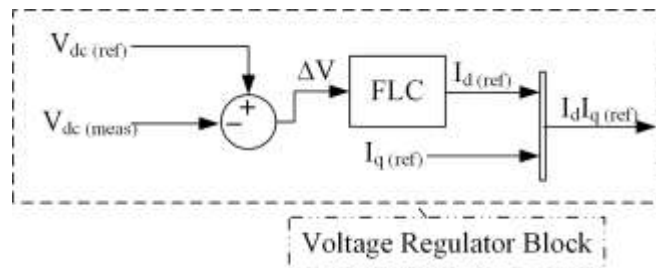


Fig. 5. FLC in voltage regulator block.

4.2. Fuzzy Logic Controller for regulation of dc link voltage

In present work, PI controller and FLC is implemented in voltage regulator block to minimize the error produced and to maintain dc link voltage constant with changes in load. As shown in “Fig. 5”, FLC is implemented and its output voltage response has been compared with output response of model implemented by using traditional PI controller. FLC, a nonlinear controller has gained wide popularity because of its logical response to nonlinear behaviour of the input parameters [17]. Mamdani and Tagachi-Sukeno (T-S) are two design methods available in FLC, of which Mamdani method is used in present model.

The steps involved in FLC are fuzzification, rule base with fuzzy inference system and defuzzification process [18]. Fuzzification process converts crisp input values into fuzzy membership values, then process it by fuzzy inference system as per rule base. Defuzzification process again converts back the fuzzy membership values into crisp output values [19]. The input to FLC is error ‘e’ and change in error ‘Δe’ given by (10) and (11).

$$e = V_{dc(ref)} - V_{dc(meas)} \tag{10}$$

$$\Delta e = e(k) - e(k - 1) \tag{11}$$

The error ‘e’ is the difference between the reference and measured dc link voltages represented by  $V_{dc(ref)}$  and  $V_{dc(meas)}$ . Equation (11) represents the change in error, whereas  $e(k)$  and  $e(k - 1)$  is error at  $(K)^{th}$  and  $(K - 1)^{th}$  sample times. The output of FLC is  $I_d$ , which is fed as reference d-axis current to current regulator block in order to control the active power to be produced by inverter.

Table 1. Fuzzy rule base matrix.

		Δe				
		nl	nc	zo	pc	pl
e	nl	nl	nl	nc	nc	zo
	nc	nl	nc	nc	zo	pc
	zo	nc	nc	zo	pc	pc
	pc	nc	zo	pc	pc	pl
	pl	zo	pc	pc	pl	pl

A total of 25 fuzzy rules has been used, given in “Table 1” with linguistic variables like positive large (pl), positive compact (pc), zero (zo), negative compact (nc) and negative

large (nl). The membership functions used at input and output of FLC in standalone mode and grid connected mode

of operation of PV system is shown in “Fig. 6” and “Fig. 7”.

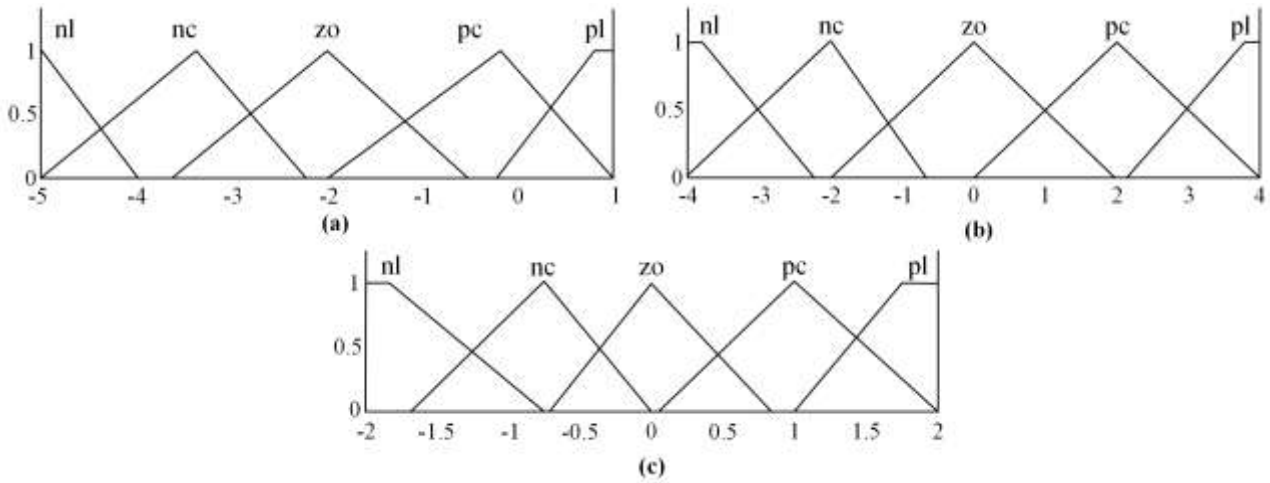


Fig. 6. Membership functions of FLC in standalone mode of operation at (a). Input ‘e’, (b). Input ‘Δe’, and (c). Output  $I_d$ .

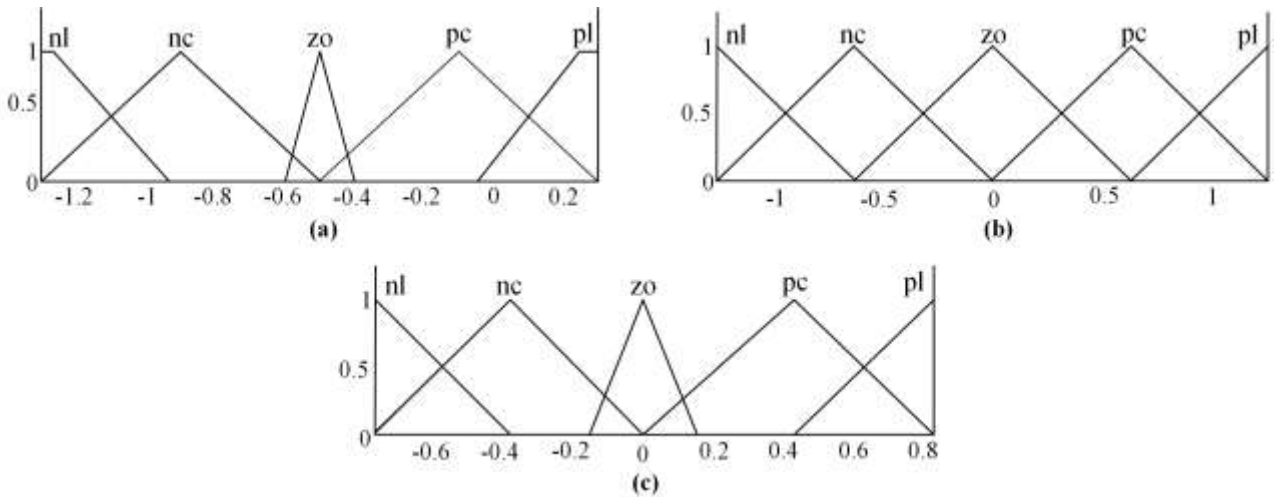


Fig. 7. Membership functions of FLC in grid connected mode of operation at (a). Input ‘e’, (b). Input ‘Δe’, and (c). Output  $I_d$ .

5. Simulation

A PV array with 14 kW and 10 kW power at output side of inverter in standalone mode and grid connected mode have been simulated in MATLAB/SIMULINK platform. The parameters of KC200GT solar PV module was used in above work, as mentioned in [11, 20] and its values are given in “Table 2”. In order to produce the required amount of power, the number of strings that has to be connected in parallel is given by  $N_{pp}$ , whereas each string will consist of  $N_{ss}$  number of series connected PV modules. The other parameters used in the implemented model of PV system is given in “Table 3”. The four models that has been simulated along with the variation in load are: PV system connected in standalone mode and grid connected mode with PI controller and FLC in Voltage Regulator block.

In standalone mode, PV array has been modelled in such a way that it will be able to supply additional power when required by load. The PV system is connected to real power

load of 5 kW during 0 to 1 seconds and an additional load of 7 kW has been connected during 1 to 2 seconds of simulation time. The behaviour of implemented model was observed at the output side of inverter while switching load from lower value to higher value and vice versa.

Table 2. KC200GT PV module parameters.

$V_{oc}$	32.9 V
$I_{sc}$	8.21 A
$a$	1.3
$K_T$	0.0032 A/K
$R_s$	0.221Ω
$R_p$	415.405 Ω
$N_s$	54
$k$	$1.3806503 \times 10^{-23} J/K$
$q$	$1.60217646 \times 10^{-19} C$

**Table 3.** Other parameters used in PV System.

Inductance of Boost Converter $L_b$	0.5 H
DC Link Capacitance	0.012 F
Nominal DC bus voltage	500 V
Inductance of Filter L	125 $\mu$ H
Resistance of Filter R	3 m $\Omega$
Transformer rating	25000/260 V, 200 KVA

In grid connected mode, the same values of load as in standalone mode has been connected to PV system in order to observe its behaviour with PI controller and FLC in voltage regulator block. Extra load of 7 kW, as in standalone mode has been applied during the simulation time of 1 to 2 secs, whereas the output power of PV array has been limited to 10 kW in order to observe power supplied by grid. The grid part of the simulated model has been implemented similar to that given in [21].

**6. Results**

The variation of I-V and P-V characteristics of PV array at different temperatures and insolation levels have been plotted in “Fig. 8” and “Fig. 9”. From “Fig. 8(a)”, it may be observed that the short circuit current of simulated PV array is 41 A and the open circuit voltage is 390 V at nominal temperature conditions. At the same time, similar output values may be found at nominal insolation conditions as shown in “Fig. 8(b)”. With the increase in temperature, there was decrease in maximum voltage generated, which directly effects the maximum power generated by PV system as shown in “Fig. 8(a)” and “Fig. 9(a)”.

The effect in maximum power generated may also be observed from “Fig. 8(b)” and “Fig. 9(b)”, that whenever there is decrease in insolation level from its nominal value, the maximum current to be generated by PV array will decrease. Identical output parameters has been plotted for all of the simulated models.

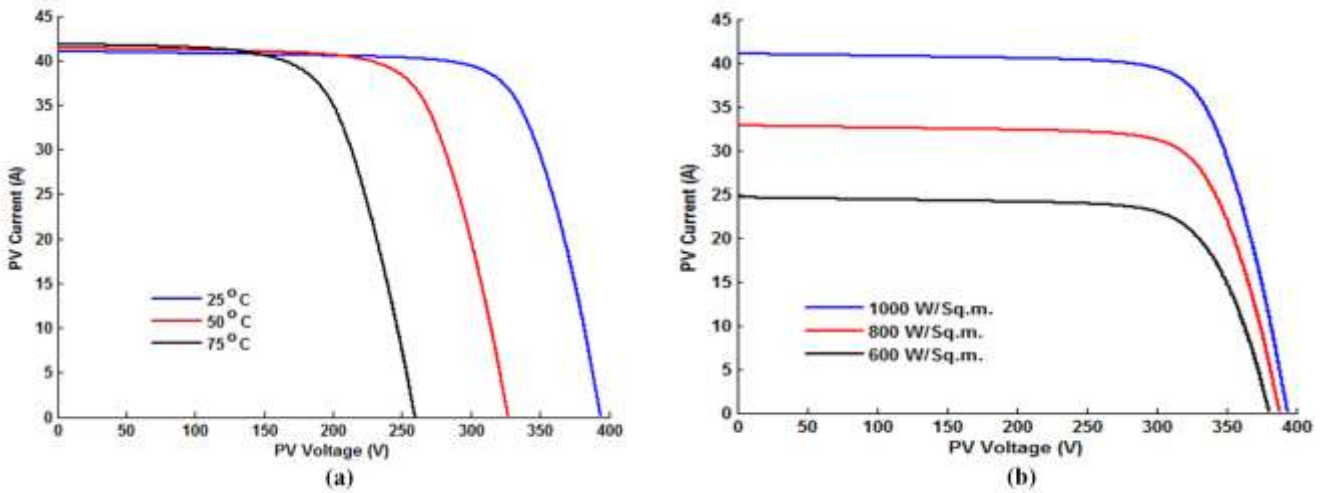


**Fig. 8.** Variation of I-V characteristics at different (a). Temperature levels and (b). Insolation levels.

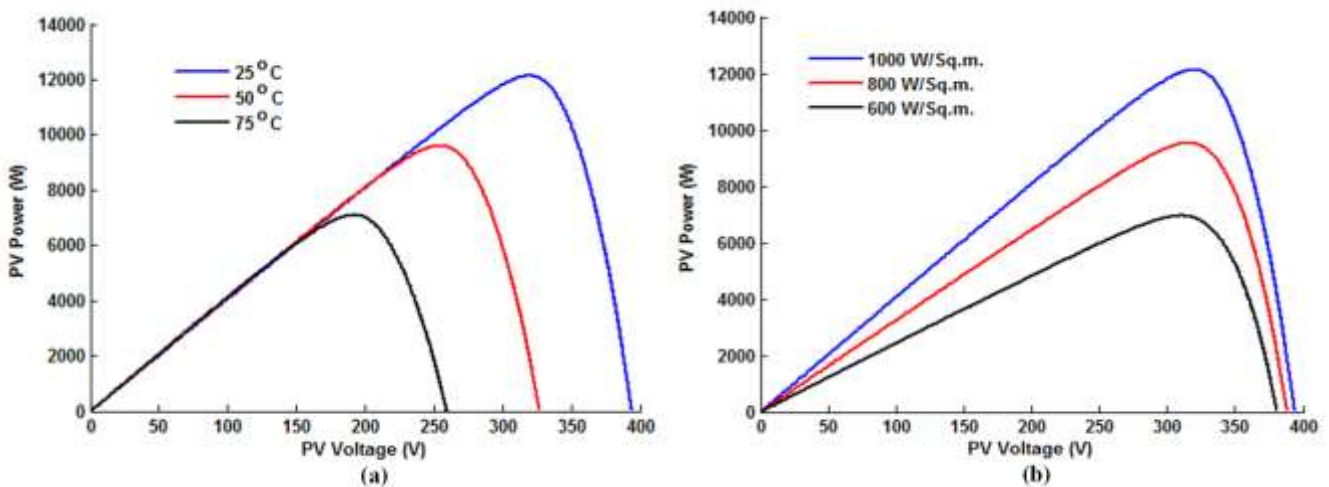


**Fig. 9.** Variation of P-V characteristics at different (a). Temperature levels and (b). Insolation levels.

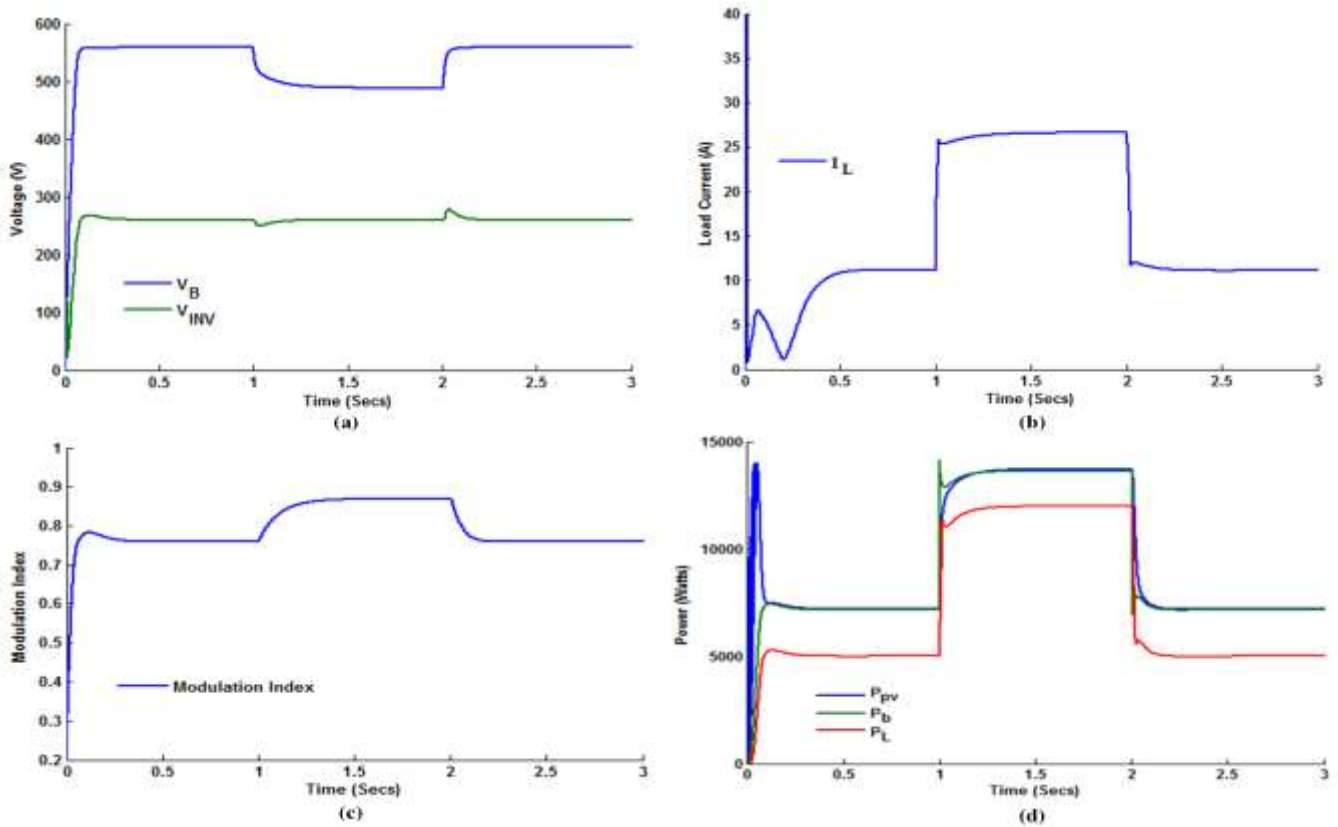


**Fig. 10.** Output characteristics of PV system in standalone mode with PI controller in voltage regulator block (a).Voltage curves of boost converter and inverter (in rms) (b). Load current (in rms) (c). Variation of modulation index (d). Power curves.

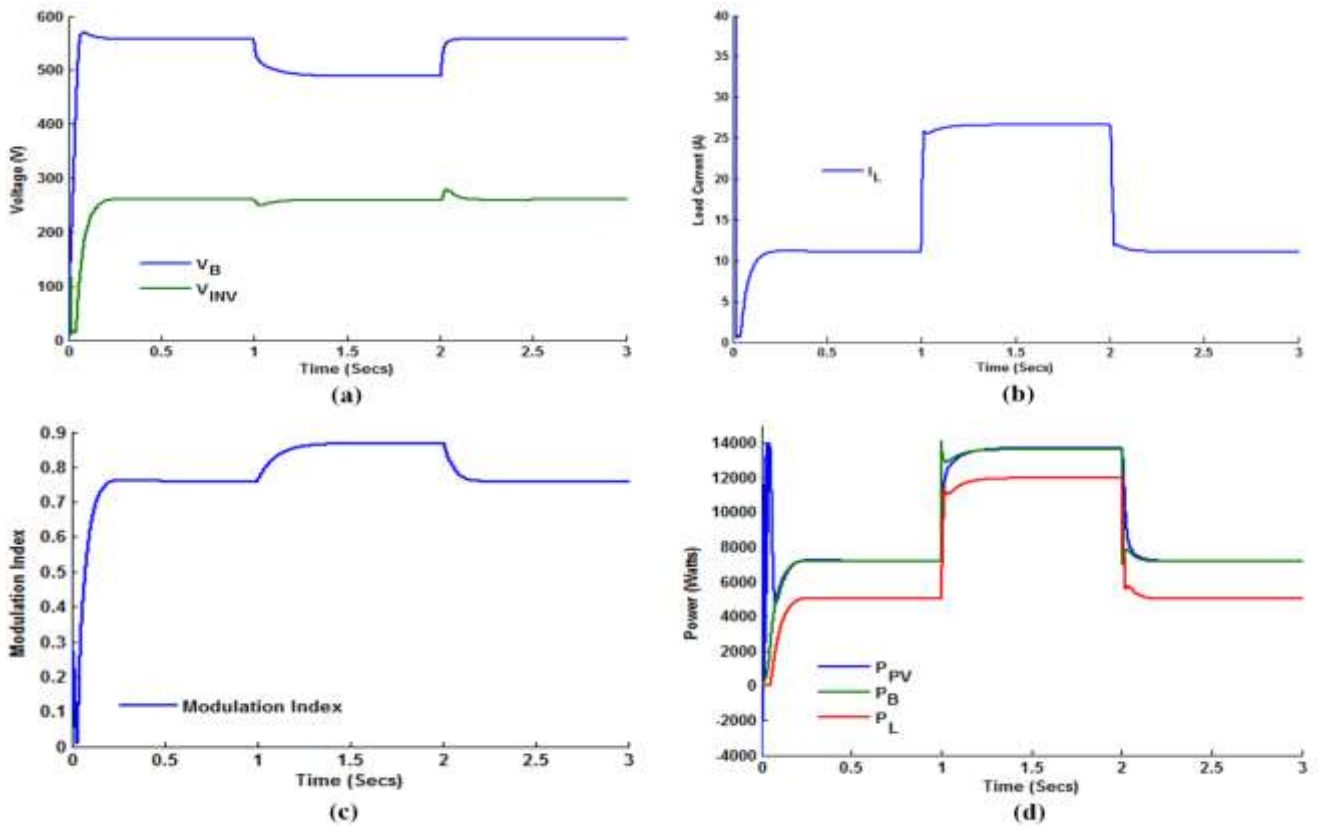


**Fig. 11.** Output characteristics of PV system in standalone mode with FLC in voltage regulator block (a).Voltage curves of boost converter and inverter (in rms) (b). Load current (in rms) (c). Variation of modulation index (d). Power curves.

At the instant of starting in standalone mode operation of PV system with PI controller in voltage regulator block and at a nominal load of 5 kW, it may be observed that the delay time of voltage, current and power is approximately 0.6 secs which is shown in “Fig. 10(a)”, “Fig. 10(b)” and “Fig. 10(d)”. During switching on of an additional 7 kW load, the time taken to supply adequate amount of power is 0.71 secs which has been shown in “Fig.10 (d)”. At the same time, it may be observed that there is decrease in dc link voltage at the input side of inverter but the output voltage remains constant due to increase in the value of modulation index as shown in “Fig.10(a)” and “Fig. 10(c)”. As soon as the additional load is switched off, the time taken by the voltage and power to settle down is 0.4 secs.

“Figure 11” shows the output characteristics of PV system connected in standalone mode of operation with FLC

in voltage regulator block. The output response is same as that of PV system in standalone mode with PI controller in voltage regulator block but the only difference is that the transient time is very less in this case. The time taken by the system at the instant of starting to settle down the transients is 0.25 secs which is very less as compared to the previous model as shown in “Fig. 11(a)”, “Fig. 11(b)” and “Fig. 11(d)”. After changing the load from 5 kW to 12 kW, the time taken to settle down the transients is 0.3 secs and after switching off the additional load, the transient duration is only 0.1 secs. In case of FLC based model there are less disturbances and the convergence to a new value is very smoother and quick in nature which may be observed in “Fig. 12”.

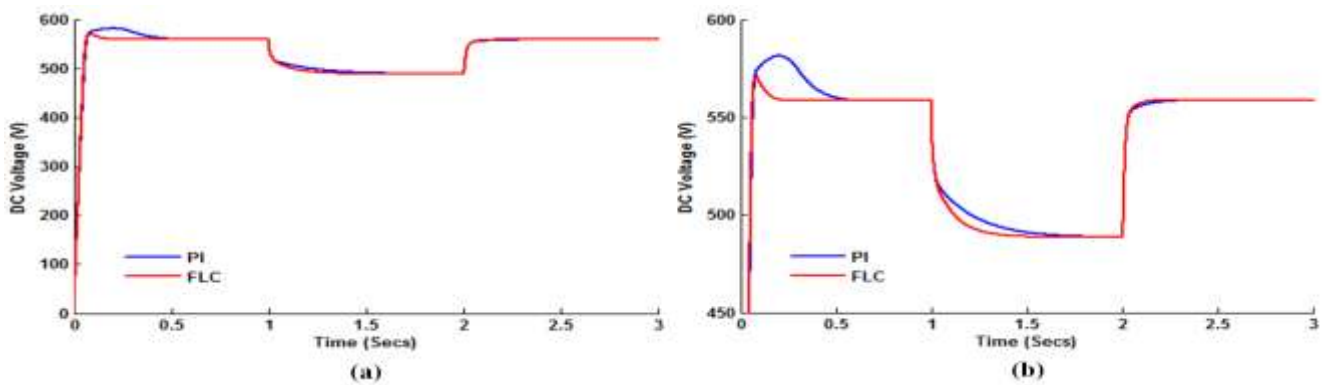


Fig. 12. (a) Comparison of output voltages of dc boost converter with PI controller and FLC in standalone mode of operation, (b). Transients in voltages.

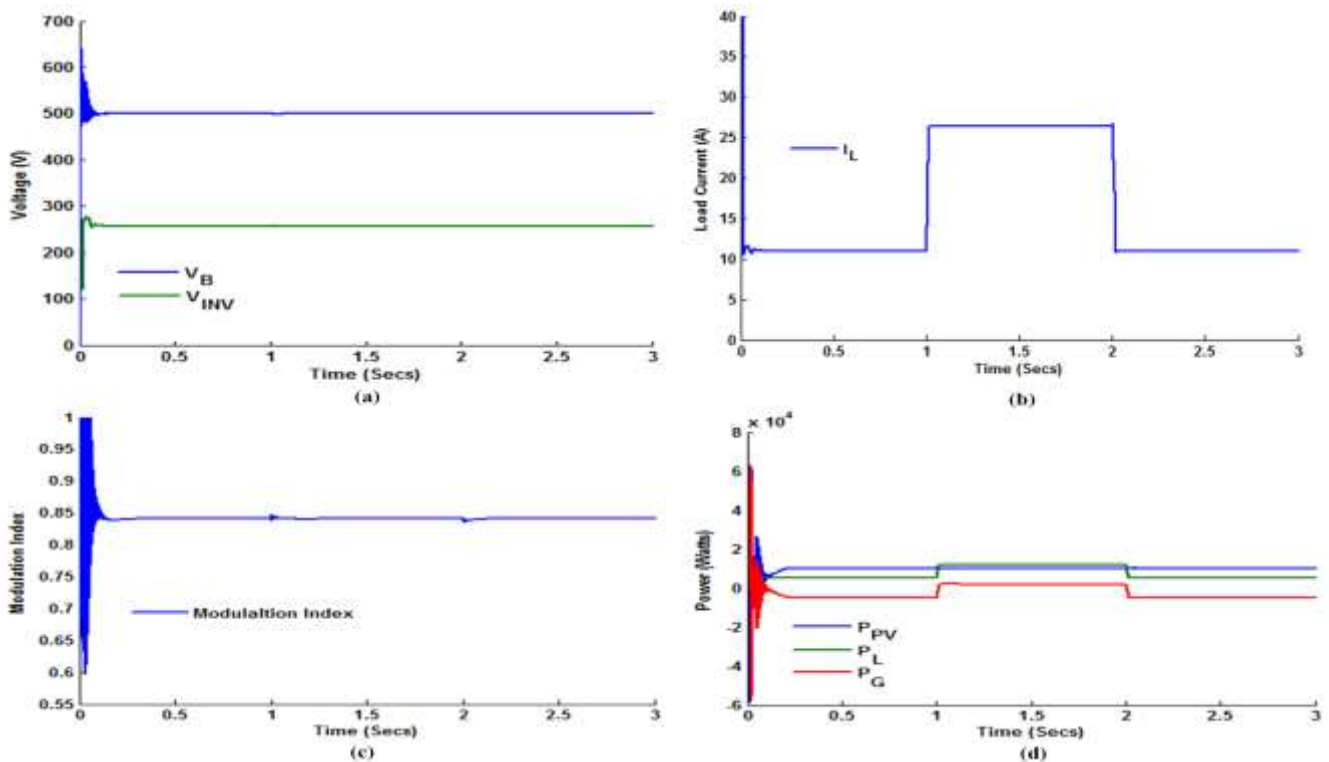
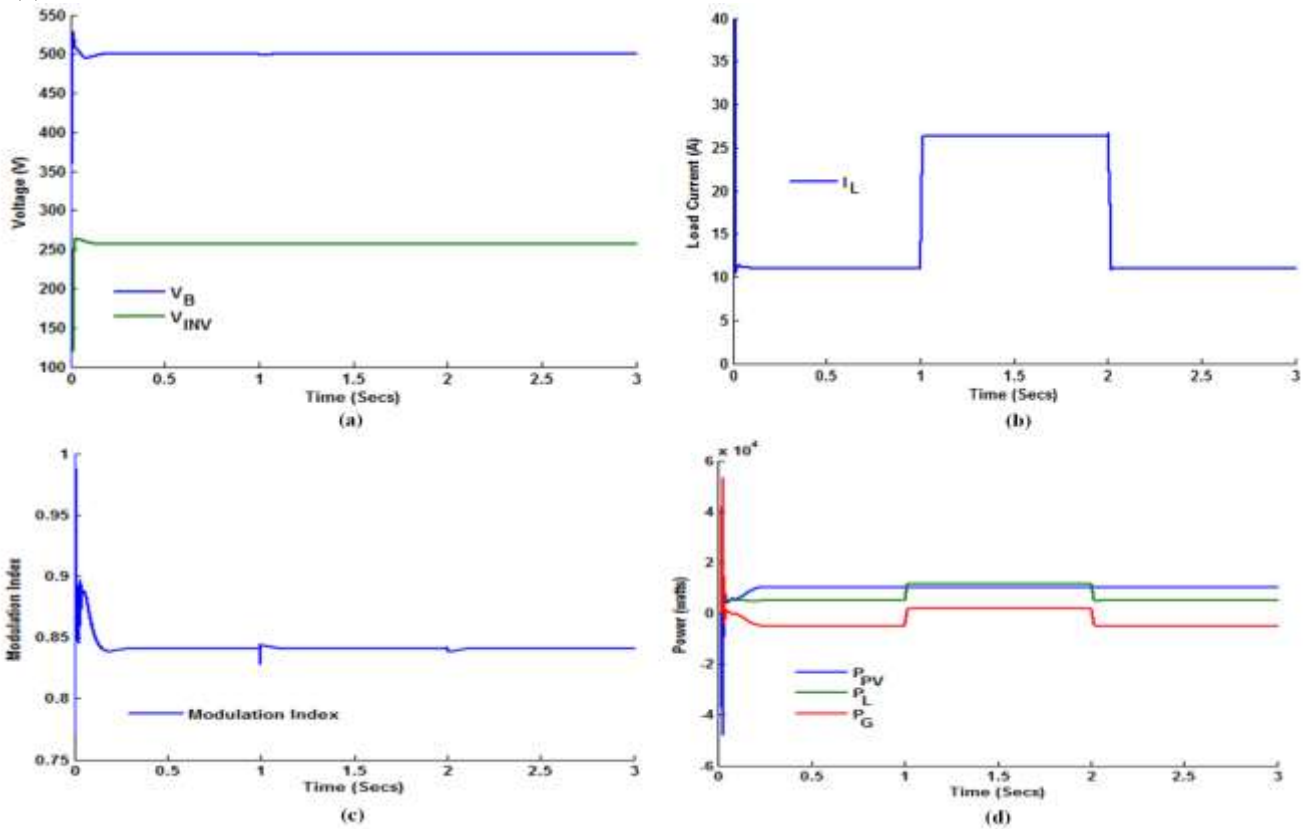


Fig. 13. Output characteristics of PV system in grid connected mode with PI controller in voltage regulator block; (a).Voltage curves of boost converter and inverter (in rms), (b). Load current (in rms), (c). Variation of modulation index, (d). Power curves.

The output characteristic of PV system in grid connected mode with conventional PI controller employed in voltage regulator block is shown in “Fig. 13”. In “Fig. 13(a)”, it has been observed that boost converter and inverter voltages remain constant when the load value is increased from 5 kW to 12 kW during 1 to 2 secs. Effect of increased load on modulation index is very less due to constant dc link voltage as shown in “Fig. 13(c)”, whereas transients at the instant of starting is more. When compared to earlier model in standalone mode of operation, the dc link voltage does not decrease at the input side of inverter but in case of load current, it has been found that there is large disturbance due to connected load at the instant of starting as shown in “Fig. 13(b)”.

“Figure 13(d)” shows that PV array is supplying a constant output power of 10 kW, out of which 5 kW is drawn by the load and rest 5 kW is supplied to grid during 0 to 1 secs and 2 to 3 secs of simulation time which may be observed from the negative value (-5 kW) of the curve  $P_G$ . During 1 to 2 secs, a load of 12 kW has been connected, but PV system is capable of supplying only 10 kW power and the rest 2 kW power required by load is drawn from the grid. It is also observed that when additional load of 7 kW is connected, there is small transient in the output voltage of boost converter and time taken by the transient to settle down is 0.1 seconds (which may be observed between 1 to 1.2 seconds).



**Fig. 14.** Output characteristics of PV system in grid connected mode with FLC in voltage regulator block; (a). Voltage curves of boost converter and inverter (in rms), (b). Load current (in rms), (c). Variation of modulation index, (d). Power curves.

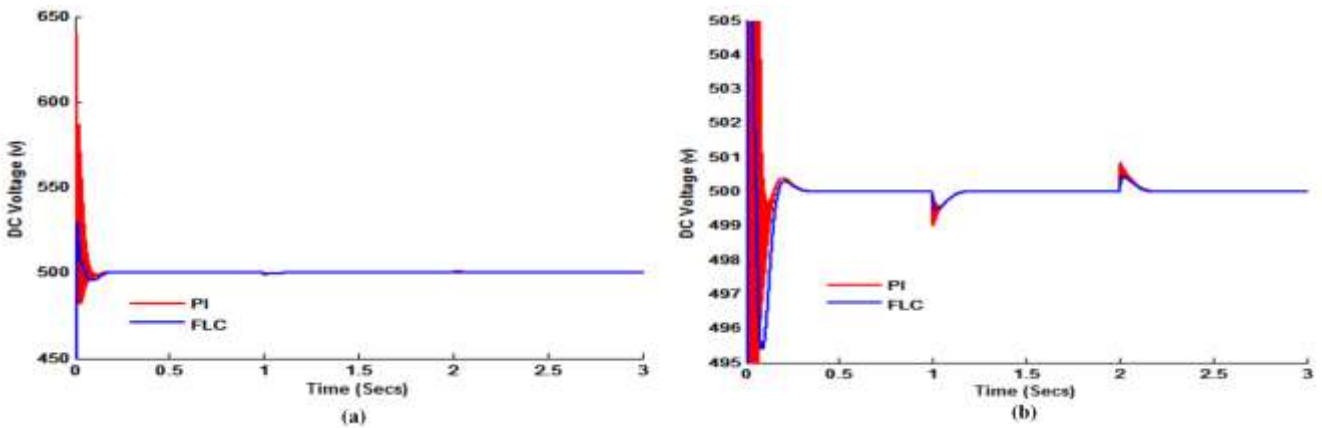


**Fig. 15.** (a) Comparison of output voltages of dc boost converter with PI controller and FLC in grid connected mode of operation, (b). Transients in voltages.

Instead of PI controller, FLC was employed in voltage regulator block and the observations are shown in “Fig.14”. From “Fig. 14(a)”, it has been observed that there is less transients in output voltages of boost converter and inverter at the instant of starting. When compared to earlier model, the duration of transients in load current and modulation index is very less as observed in “Fig. 14(b)” and “Fig. 14(c)” which is in the range of 0.12 secs at the instant of starting, 0.08 secs at the instant of switching on of an additional load and 0.07 secs when the additional load is removed. The output current and power curves are also smoother in nature with less transients during switching on of an additional 7 kW load.

The comparison of output voltages of dc boost converter with PI controller and FLC based voltage regulator block is shown in “Fig. 15” and it has been found that transients in output voltage of boost converter due to FLC based voltage regulator block is very less and voltage settles down very smoothly.

The transient time of all the four simulated models at different positions are given in “Table 4”, which itself explain the merit of FLC based models.

**Table 4.** Transient time at different positions of PV system.

Type of model	Transient time in secs at different positions		
	At the instant of starting	When the additional load is switched on	When the additional load is switched off
I. Standalone mode of operation of PV system			
a. With PI controller in voltage regulator block	0.71	0.65	0.4
b. With FLC in voltage regulator block	<b>0.25</b>	<b>0.3</b>	<b>0.1</b>
II. Grid connected mode of operation of PV system			
a. With PI controller in voltage regulator block	0.22	0.1	0.1
b. With FLC in voltage regulator block	<b>0.12</b>	<b>0.07</b>	<b>0.08</b>

## 7. Conclusion

In this paper, four models of PV system has been simulated to study its behaviour during switching on of an additional load, in addition to an existing load in standalone mode and sharing of load between PV System and grid in grid connected mode of operation. Mamdani approach based Fuzzy logic controller with 25 rule base system has been employed in voltage regulator block resulting in better performance than the traditional PI controller. The voltage characteristics at the output of boost converter and inverter has been plotted for PI controller and FLC based voltage regulator block in order to conclude that the transients in later model is very less and also the dc link voltage follow its reference value very smoothly.

The transient time in FLC based models is very less at the instant of starting, during switching on of an additional load and after removing the additional load which has been observed by plotting different output characteristics. In case of PV system connected in standalone mode, it has been observed that there is an increase in the value of modulation index of an inverter due to decrease in dc link voltage during switching on of an additional load whereas in case of PV system operated in grid connected mode, the modulation index value settles down to its original value because of stronger support of grid voltage.

## References

- [1] S. M. Mirhassani, H. C. Ong, W.T.Chong, K.Y.Leong, “Advances and Challenges in grid tied photovoltaic systems”, Renewable and Sustainable Energy Reviews, Vol. 49, pp. 121–131, 2015.
- [2] B. N. Alajmi, K. H. Ahmed, G. P. Adam and B. W. Williams, “Single-Phase Single-Stage Transformer less Grid-connected PV system”, IEEE Transactions on Power Electronics, Vol. 28, No. 6, pp. 2664–2676, 2013.
- [3] D. Verma, S. Nema, A. M. Shandilya, S. K. Dash, “Maximum power point tracking (MPPT) techniques: Recapitulation in solar photovoltaic systems”, Renewable and Sustainable Energy Reviews, Vol. 54, pp. 1018–1034, 2016.
- [4] B. Subudhi, R. Pradhan, “A Comparative Study on Maximum Power Point Tracking Techniques for Photovoltaic Power Systems”, IEEE Transactions on Sustainable Energy, Vol. 4, No. 1, January 2013, pp. 89 - 98.
- [5] S. Lyden, M. E. Haque, “Maximum Power Point Tracking techniques for photovoltaic systems: A comprehensive review and comparative analysis”, Renewable and Sustainable Energy Reviews, Vol.52 (2015), pp.1504–1518.
- [6] N. Femia, G. Petrone, G. Spagnuolo, M. Vitelli, “Optimization of Perturb and Observe Maximum Power Point Tracking Method”, IEEE Transactions on Power Electronics, Vol. 20, No. 4, 2005.

- [7] F. Liu, S. Duan, F. Liu, B. Liu, Y. Kang, "A Variable Step Size INC MPPT Method for PV Systems", IEEE Transactions on Industrial Electronics, Vol. 55, No. 7, pp. 2622–2628, 2008.
- [8] L. Liu, X. Meng, C. Liu, "A review of maximum power point tracking methods of PV power system at uniform and partial shading", Renewable and Sustainable Energy Reviews, Vol. 53, pp. 1500–1507, 2016.
- [9] A. Menadi, S. Abdeddaim, A. Ghamri, A. Betka, "Implementation of fuzzy-sliding mode based control of a grid connected photovoltaic system", ISA Transactions, Vol. 58, pp. 586–594, 2015.
- [10] M. A. Mahmud, H. R. Pota, and M. J. Hossain, "Dynamic Stability of Three-Phase Grid-Connected Photovoltaic System Using Zero Dynamic Design Approach", IEEE Journal of Photovoltaics, Vol. 2, No. 4, pp. 564–571, 2012.
- [11] M. G. Villalva, J. R. Gazoli, and E. R. Filho, "Comprehensive Approach to Modeling and Simulation of Photovoltaic Arrays", IEEE Transactions on Power Electronics, Vol. 24, No. 5, pp. 1198–1208, 2009.
- [12] K. Ishaque, Z. Salam, Syafaruddin, "A comprehensive MATLAB Simulink PV system simulator with partial shading capability based on two-diode model", Solar Energy, Vol. 85, pp. 2217–2227, 2011.
- [13] A. A. Nabulsi, R. Dhaouadi, "Efficiency Optimization of a DSP-Based Standalone PV System Using Fuzzy Logic and Dual-MPPT Control", IEEE Transactions on Industrial Informatics, Vol. 8, No. 3, pp. 573–584, 2012.
- [14] G. Dileep, S. N. Singh, "Maximum power point tracking of solar photovoltaic system using modified perturbation and observation method", Renewable and Sustainable Energy Reviews, Vol. 50, pp. 109–129, 2015.
- [15] S. K. Kollimalla, M. K. Mishra, "Variable Perturbation Size Adaptive P&O MPPT Algorithm for Sudden Changes in Irradiance", IEEE Transactions on Sustainable Energy, Vol. 5, No. 3, pp. 718–728, July 2014.
- [16] M. A. A. M. Zainuri, M. A. M. Radzi, A. C. Soh, N. A. Rahim, "Development of adaptive perturb and observe-fuzzy control maximum power point tracking for photovoltaic boost dc–dc converter", IET Renewable Power Generation, Vol. 8, No. 2, pp. 183–194, 2014.
- [17] S. Choudhury, P. K. Rout, "Adaptive Fuzzy Logic Based MPPT Control for PV System under Partial Shading Condition", International Journal of Renewable Energy Research, Vol.5, No. 4, pp. 1252–1263, 2015.
- [18] I. H. Altasa, A. M. Sharaf, "A novel maximum power fuzzy logic controller for photovoltaic solar energy systems", Renewable Energy, Vol. 33, pp. 388–399, 2008.
- [19] T. J. Ross, Fuzzy control with Engineering applications, 2nd ed, Wiley student edition, John Wiley & Sons (Asia) Pte.LTd., Singapore.
- [20] Kyocera KC200GT solar array datasheet. Available at: <http://www.kyocera.com.sg/products/solar/pdf/kc200gt.pdf> last visit date: 05<sup>th</sup> November, 2016.
- [21] <https://in.mathworks.com/matlabcentral/fileexchange/34752-grid-connected-pv-array> last visit date: 01<sup>st</sup> November 2016.